

Linking three-dimensional core-collapse supernova simulations with observations

Annop Wongwathanarat^{1,2}

¹RIKEN, Astrophysical Big Bang Laboratory, 2-1 Hirosawa, Wako, Saitama 351-0198, Japan
email: annop.wongwathanarat@riken.jp

²Max-Planck-Institut für Astrophysik, Karl-Schwarzschild-Str. 1, 85748 Garching, Germany

Abstract. To understand a wide variety of properties of young core-collapse supernova (CCSN) remnants being revealed by modern observations three-dimensional simulations of CCSNe starting from the initiation of the explosion until the expanding stellar debris transform into gaseous remnants are needed. We briefly review recent progress in modeling CCSNe on a long time scale. A current effort to model bolometric light curves based on 3D CCSN explosion models for comparison with observational data from SN 1987A is also discussed.

Keywords. supernovae: general, supernovae: individual (Supernova 1987A), hydrodynamics, instabilities

1. Introduction

Multi-wavelength observations of nearby young CCSN remnants, e.g. Crab, Cassiopeia A, and SN 1987A, reveal large scale asymmetries and complex structures of different chemical elements in the expanding stellar debris. Because interactions between ejecta and circumstellar materials are still minimal for young remnants these observations immediately suggest that the explosions were not spherically symmetric. Origins of asymmetries which influence the final observed morphology of remnants include asymmetries in the progenitor core prior to core collapse (Arnett & Meakin 2011; Couch *et al.* 2015; Müller *et al.* 2016), hydrodynamic instabilities such as convection (e.g., Herant *et al.* 1994) and the standing accretion shock instability (SASI, Fogliizzo 2002; Blondin *et al.* 2003; Blondin & Mezzacappa 2006) which occur during the shock revival phase, and secondary mixing (e.g. Rayleigh-Taylor and Richtmyer-Meshkov) instabilities triggered by the SN shock propagation through the onion shell structure of the progenitor star (Chevalier 1976; Kifonidis *et al.* 2006). Therefore, to make a direct comparison of the ejecta asymmetries, which is one of the many CCSN observables besides neutrinos, gravitational waves, nucleosynthesis yields, remnant properties, light curves, and spectra, between CCSN models and observations it is unavoidable that the models must consider the development of asymmetries in different stages of CCSN explosions and their complex interplays consistently.

Undoubtedly, performing a numerical simulation of CCSN explosions which considers the core collapse through the shock revival phase until the SN ejecta expand and transform into a gaseous nebula is an extremely difficult task. Apart from big hurdles in modeling the core of massive stars before collapse and the initiation of the explosions in multi dimensions, carrying out long-time simulations tracing the explosion asymmetries from the moment after the SN shock resumes its outward propagation until it breaks out of the surface of the progenitor star also requires a huge computational demand because of the massive length- and timescales needed to be covered by these simulations. Here,

we give a short review of progress in simulating three-dimensional (3D) long-time CCSN explosions and discuss how the outcomes of these simulations be used in connection with one-dimensional (1D) light curve modeling to constrain the structure of the progenitor star in the case of SN 1987A.

2. Progress on long-time simulations of CCSNe

After the explosion of SN 1987A on February 23, 1987 a large number of two-dimensional (2D) simulations studying the growth of Rayleigh-Taylor instabilities (RTIs) while the SN shock plows through shells of elements inside the progenitor star have been performed. An extensive list of references to such works was already given in, e.g., Wongwathanarat *et al.* (2015) and Mao *et al.* (2015). One of the main goals of these simulations was to explain the mechanism which facilitates outward mixing of the radioactive nickel synthesized deep inside the SN core into the hydrogen rich envelope and inward mixing of hydrogen into the helium rich layer. Such large-scale radial mixing was implied following analyses of observational data obtained from SN 1987A such as early detections of hard X-ray (Dotani *et al.* 1987; Sunyaev *et al.* 1987) and gamma-ray lines (Matz *et al.* 1988), a high-velocity feature in the [Fe II] line at ~ 3500 km/s (Haas *et al.* 1990), and the 1D light curve modeling by radiation hydrodynamic calculations (Woosley 1988; Shigeyama & Nomoto 1990; Blinnikov *et al.* 2000; Utrobin 2004). It turned out that RT mixing seeded by small-scales random perturbations in 2D models initiated by point-like or piston-driven explosions was insufficiently vigorous to carry out nickel to high velocities beyond ~ 3000 km/s as required by observations, unless an asymmetric or jet-like explosion is assumed (e.g., Nagataki *et al.* 1998; Nagataki 2000). This problem was termed the “nickel discrepancy” by Herant & Benz (1992).

The number of attempts to perform 3D calculations investigating the growth of RTIs in the SN envelope is much smaller than 2D studies. Nagasawa *et al.* (1988) made the first advance to the third dimension by performing 3D models of point-like explosions in $n = 3$ polytropes using smoothed particle hydrodynamics (SPH). A motivation for Nagasawa *et al.* (1988) was that non-axisymmetric modes of RTIs which could not be captured by 2D calculations can be present in 3D. They reported fast growth of RTIs which can explain the early rise of X-rays observed in SN 1987A, but Muller *et al.* (1989) who did a similar 3D calculation with a grid-based code contradicted their results. Kane *et al.* (2000) made a comparison of RT growth rate of single-mode perturbation in 2D and 3D, and found that the perturbation grows $\sim 30\%$ faster in a 3D calculation. This result was later tested by Joggerst *et al.* (2010). Nevertheless, the conclusion made by Joggerst *et al.* (2010) was different. They concluded that RTIs grow faster in 3D only initially. But, soon after RT fingers begin to interact and merge the growth rate decreases. As a result the extent of the fluid mixing zone is similar in 2D and 3D calculations. Hungerford *et al.* (2003) and Hungerford *et al.* (2005) re-investigated effects of asymmetric explosions on the extent of RT mixing and the resulting emergence of gamma-rays lines. They claimed that single-lobe explosions can explain the redshifted high-velocity component of the iron line observed in SN 1987A. The 3D calculation which followed the development of RTIs for the longest time was reported by Ellinger *et al.* (2012). They studied properties of clumped ejecta caused by fragmentations due to RTIs and their evolution until ~ 30 years after the explosion.

All of the studies mentioned above, however, neglected detailed explosion physics which is, in fact, very crucial in determining the ejecta asymmetries at late times. The calculations instead relied on simple methods to drive explosions. Using a different approach to initiate the explosion Kifonidis *et al.* (2003) and Kifonidis *et al.* (2006) were the first

to model both the neutrino-driven explosion engine and the subsequent evolution of the SN shock until shock breakout in 2D. Modeling the explosions starting from core bounce in multi-D allowed them to capture the development of low-mode convective instabilities and SASI in their calculations. These explosion asymmetries act as large-scale large-amplitude perturbations for secondary RTIs at composition shell interfaces to grow strongly.

The importance of the 3D geometry and the development of low-mode instabilities in the explosion engine on the growth of secondary RTIs were both taken into account in the work by Hammer *et al.* (2010). They demonstrated that a 3D calculation of a neutrino-driven explosion starting from shortly after core bounce can provide a solution for the nickel discrepancy. They reported the asymptotic velocities of nickel-rich clumps up to ~ 4500 km/s in their 3D model, which are much higher velocities than in 2D calculations that they performed. They explained the 2D-3D difference in the velocity distribution of nickel at shock breakout by a simple geometrical argument. In 2D geometry a nickel rich clump in the simulation assumes a torus-like structure because of the axially symmetric constraint. Thus it experiences larger drag force in comparison with a spherical-like clump in 3D geometry.

The result obtained by Hammer *et al.* (2010) was different from that of Joggerst *et al.* (2010). However, their results, in fact, do not contradict each other. Because Joggerst *et al.* (2010) initiate the explosions using pistons and let RTIs develop from small-scale random perturbations, numerous small RT fingers grow and interact with each other. In contrast, only a few nickel-rich RT fingers develop in the 3D calculation of Hammer *et al.* (2010). These fingers grow from large-scale large-amplitude perturbations created by neutrino-driven convection and SASI during the first second of the explosion, and they propagate independently in different directions.

The work by Hammer *et al.* (2010) was a big step toward long-time modeling of neutrino-driven CCSNe in 3D. Still, they only investigated one $15 M_{\odot}$ blue supergiant progenitor by Woosley *et al.* (1988). The growth of RTIs at shell interfaces depends greatly on the progenitor structure too, as shown by Herant & Benz (1991) in their 2D calculations in two different progenitor stars. Wongwathanarat *et al.* (2015) continued along the line of the work by Hammer *et al.* (2010), adding a progenitor dependence study. They performed a set of 3D simulations of CCSNe until ~ 1 day after the explosions for four different progenitor stars; two $15 M_{\odot}$ red supergiant stars by Woosley & Weaver (1995) and Limongi *et al.* (2000), a $20 M_{\odot}$ blue supergiant progenitor (Shigeyama & Nomoto 1990), and also the $15 M_{\odot}$ blue supergiant star by Woosley *et al.* (1988) which was used in the study of Hammer *et al.* (2010).

Indeed, Wongwathanarat *et al.* (2015) found great differences in the morphology of the nickel-rich ejecta at shock breakout between cases of different progenitors. In red supergiants, RTIs develop extremely vigorously at the He/H composition interface due to a very steep density gradient there. In addition, a very strong reverse shock forms at that interface. The reverse shock travels backward in mass coordinates and compresses the trailing nickel-rich ejecta into a very thin layer. After being compressed the nickel-rich ejecta fragments into numerous small clumps.

The dynamics of the forward shock, reverse shock, and nickel-rich ejecta is different in the case of blue supergiant progenitors. In fact, it is also different even among the two blue supergiant stars that were considered. The simulations of the $20 M_{\odot}$ star by Shigeyama & Nomoto (1990) showed much less vigorous growth of RTIs, at both C+O/He and He/H interfaces. In contrast, RTIs grows strongly at C+O/He interface in the $15 M_{\odot}$ by Woosley *et al.* (1988). Consequently, the nickel-rich ejecta penetrate through the He shell quickly and thus later can avoid being drastically decelerated by the reverse

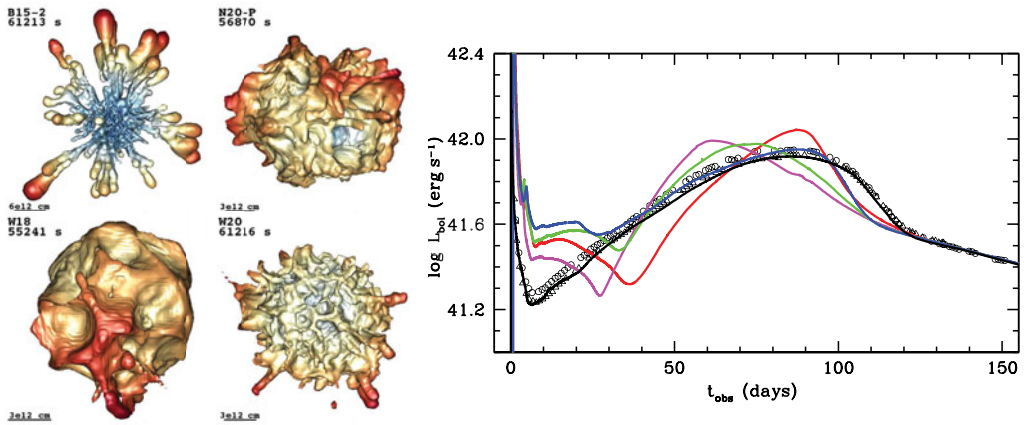


Figure 1. Morphological structures of nickel-rich ejecta in 3D simulations of Wongwathanarat *et al.* (2015) and Utrobin *et al.* (2015) and their corresponding bolometric light curves calculated by 1D radiation Lagrangian hydrodynamic code CRAB. The model B15-2 (upper left) yields a light curve with a wide dome shape (blue line) which is in good agreement with the observed data from SN 1987A during day $\sim 40 - 100$. The black solid line corresponds to the bolometric light curve of an optimal model calculated with a non-evolutionary progenitor star by Utrobin (2005).

shock, partially because of a mild acceleration of the SN forward shock. As a result the morphology of the nickel-rich ejecta resulting from this model looks unique, consisting of many elongated RT fingers. In summary, the ejecta asymmetries at shock breakout can depend very sensitively on the density structure of the progenitor star.

3. 1D light curve modeling based on 3D explosion models: the case of SN 1987A

All previous studies on light curve comparison with observations of SN 1987A have relied on models of CCSN explosions that are initiated in 1D. To reproduce the smooth rise and the wide dome-shaped light curve of SN 1987A during days $\sim 10 - 120$ outward mixing of radioactive nickel and inward mixing of hydrogen have to be introduced artificially (e.g., Utrobin 2005). Recently, Utrobin *et al.* (2015) made the first attempt to calculate bolometric light curves in 1D based on angular-averaged 3D explosion models which are evolved from shortly after core bounce until shock breakout. This light curve modeling approach eliminates the need to introduce artificial mixing within the SN ejecta because mixing is already captured in 3D hydrodynamic calculations of the SN explosions.

Utrobin *et al.* (2015) consider 3D explosion models of four different blue supergiant progenitors: two of which were calculated by Wongwathanarat *et al.* (2015). The computed bolometric light curves are compared to observational data of SN 1987A. They found that one of their models, model B15-2, yields a light curve with a broad dome shape which is in good agreement with observational data during day $\sim 40 - 120$. In all other models, the resulting light curves are either peak-like or a dome-shaped not wide enough. The failure to produce a wide enough dome-like light curve in these models means too short diffusion time of photons from the radioactive nickel decay chain powering the light curve, which results from insufficient outward mixing of nickel into the hydrogen envelope. The model B15-2 is based on the $15 M_{\odot}$ blue supergiant by Woosley *et al.* (1988) whose density structure allows for strong RT mixing near the C+O/He

interface (Wongwathanarat *et al.* 2015). Disappointingly, all models considered by Utrobin *et al.* (2015) do not produce a good match with the initial light curve peak observed during the first ~ 10 days of the SN explosion. This is caused by a too large radius of the progenitor star used for the calculations. Note that all of the considered progenitors are single stars, while SN 1987A may have been the result of a binary star.

Nevertheless, the results obtained by Utrobin *et al.* (2015) demonstrated an intriguing possibility to probe the density structure inside the progenitor star by light curve modeling.

4. Conclusions and Outlook

During the past decade considerable progress has been made in modeling CCSN explosions on a long time scale in three dimensions. 3D models which follow the time evolution of CCSNe from shortly after core bounce until shock breakout have become feasible (e.g., Hammer *et al.* 2010; Wongwathanarat *et al.* 2015). They revealed that morphology of the ejecta, especially the ejecta that are rich in heavy elements synthesized during the explosions, can depend sensitively on the density structure of the progenitor star. These 3D models already allow for a direct link between CCSN models and observations, e.g., through the 1D bolometric light curve modeling (Utrobin *et al.* 2015). Evolving 3D explosion models until decades or centuries after the explosion is currently a work in progress (Gabler *et al.*, these proceedings).

One of the major uncertainties in modeling CCSNe is the lack of a 3D model of the core of a massive star before collapse. So far, 3D simulations of CCSNe have relied solely on 1D models computed by stellar evolution codes. Asymmetries in convective shell burning during last minutes before core collapse can influence the explosion dynamics and thus may also affect the explosion asymmetries (e.g., Müller *et al.* 2016). 3D modeling of the core of massive stars is still in its infancy stage. There have been only two such calculations by Couch *et al.* (2015) and Müller *et al.* (2016) for a $15 M_{\odot}$ and a $18 M_{\odot}$ progenitor. More progenitor models are urgently needed.

References

- Arnett, W. D. & Meakin, C. 2011, *ApJ*, 733, 78
Blinnikov, S., Lundqvist, P., Bartunov, O., Nomoto, K., & Iwamoto, K. 2000, *ApJ*, 532, 1132
Blondin, J. M. & Mezzacappa, A. 2006, *ApJ*, 642, 401
Blondin, J. M., Mezzacappa, A., & DeMarino, C. 2003, *ApJ*, 584, 971
Chevalier, R. A. 1976, *ApJ*, 207, 872
Couch, S. M., Chatzopoulos, E., Arnett, W. D., & Timmes, F. X. 2015, *ApJ* (Letters), 808, L21
Dotani, T., Hayashida, K., Inoue, H., Itoh, M., & Koyama, K. 1987, *Nature*, 330, 230
Ellinger, C. I., Young, P. A., Fryer, C. L., & Rockefeller, G. 2012, *ApJ*, 755, 160
Foglizzo, T. 2002, *A&A*, 392, 353
Haas, M. R., Erickson, E. F., Lord, S. D., *et al.* 1990, *ApJ*, 360, 257
Hammer, N. J., Janka, H.-T., & Müller, E. 2010, *ApJ*, 714, 1371
Herant, M. & Benz, W. 1991, *ApJ* (Letters), 370, L81
Herant, M. & Benz, W. 1992, *ApJ*, 387, 294
Herant, M., Benz, W., Hix, W. R., Fryer, C. L., & Colgate, S. A. 1994, *ApJ*, 435, 339
Hungerford, A. L., Fryer, C. L., & Rockefeller, G. 2005, *ApJ*, 635, 487
Hungerford, A. L., Fryer, C. L., & Warren, M. S. 2003, *ApJ*, 594, 390
Joggerst, C. C., Almgren, A., & Woosley, S. E. 2010, *ApJ*, 723, 353
Kane, J., Arnett, D., Remington, B. A., *et al.* 2000, *ApJ*, 528, 989
Kifonidis, K., Plewa, T., Janka, H., & Müller, E. 2003, *A&A*, 408, 621

- Kifonidis, K., Plewa, T., Scheck, L., Janka, H.-T., & Müller, E. 2006, *A&A*, 453, 661
- Limongi, M., Straniero, O., & Chieffi, A. 2000, *ApJS*, 129, 625
- Mao, J., Ono, M., & Nagataki, S., et al. 2015, *ApJ*, 808, 164
- Matz, S. M., Share, G. H., Leising, M. D., Chupp, E. L., & Vestrand, W. T. 1988, *Nature*, 331, 416
- Muller, E., Hillebrandt, W., Orio, M., et al. 1989, *A&A*, 220, 167
- Müller, B., Viallet, M., Heger, A., & Janka, H.-T. 2016, *ApJ*, 833, 124
- Nagasawa, M., Nakamura, T., & Miyama, S. M. 1988, *PASJ*, 40, 691
- Nagataki, S. 2000, *ApJS*, 127, 141
- Nagataki, S., Shimizu, T. M., & Sato, K. 1998, *ApJ*, 495, 413
- Shigeyama, T. & Nomoto, K. 1990, *ApJ*, 360, 242
- Sunyaev, R., Kaniovsky, A., Efremov, V., et al. 1987, *Nature*, 330, 227
- Utrobin, V. P. 2004, *Astron. Lett.*, 30, 293
- Utrobin, V. P. 2005, *Astron. Lett.*, 31, 806
- Utrobin, V. P., Wongwathanarat, A., Janka, H.-T., & Müller, E. 2015, *A&A*, 581, A40
- Wongwathanarat, A., Müller, E., & Janka, H.-T. 2015, *A&A*, 577, A48
- Woodsley, S. E. 1988, *ApJ*, 330, 218
- Woodsley, S. E., Pinto, P. A., & Ensman, L. 1988, *ApJ*, 324, 466
- Woodsley, S. E. & Weaver, T. A. 1995, *ApJS*, 101, 181